Bulletin of the Geological Society of Malaysia, Volume 75, May 2023, pp. 3 - 12
DOI: https://doi.org/10.7186/bgsm75202302

A valuable approach in a quantitative seawater intrusion interpretation from the geoelectrical resistivity data for groundwater investigation in Dumai area, Indonesia

Nur Islami*, Mitri Irianti, Azhar Azhar, Muhammad Nasir, Muhammad Nor, Fakhruddin Fakhruddin, Dedi Irawan

Physics – PMIPA, Universitas Riau, Jl. HR. Soebrantas, Km. 12.5, Pekanbaru, 28293, Indonesia
* Corresponding author email address: nurislami@lecturer.unri.ac.id

Abstract: An improvement of geoelectrical resistivity interpretation has been done through this research. Up to now, the geoelectrical resistivity data was interpreted qualitatively especially in the case of the aquifer intruded by seawater, and the percentage of seawater mixture content in the aquifer cannot be predicted. In this research, a valuable approach was used in the prediction of percentage seawater mixture in the shallow aquifer that is intruded by seawater. The study was conducted in the coastal area which is mainly covered by peat soil. The research employed the direct soil resistivity measurement and the ground surface resistivity survey. Geoelectrical resistivity with the Wenner configuration was used for both measurements. The soil character and the fluid content in the soil were measured to obtain their correlation to the direct soil resistivity value. The results show that resistivity value is about 2-5 ohm.m for 50% seawater content mixture in aquifer and it increase to be 5-10 ohm.m for 25% seawater mix to freshwater in the aquifer. The increasing seawater content in the pore soil caused the decreases in resistivity value drastically. The percentage of seawater mixture in the fluid pore soil has been successfully predicted through the geoelectrical resistivity measurement on the surface.

Keywords: Seawater intrusion, geoelectrical resistivity, Dumai, groundwater

INTRODUCTION

The main groundwater problem faced in coastal areas is the occurrence of seawater intrusion into groundwater aquifers. This problem has increased to the point where it is difficult to find fresh groundwater for drinking and for daily needs (Panthi *et al*., 2022). In addition, the problem will also escalate to the sustainability of the ecosystem in the area (Basack *et al*., 2022). The occurrence of seawater intrusion towards land may be caused by overexploitation of groundwater (Alfarrah & Walraevens, 2018; Erostate *et al*., 2020; Armanuos *et al*., 2022) so that the hydrostatic pressure of the aquifer will decrease drastically. This will cause the entry of seawater into the groundwater aquifer (Prusty & Farooq, 2020). Apart from that, the presence of seawater in the aquifer can also be caused by the trapping of seawater during the sedimentation process in the past geological time interval (Baharuddin *et al*., 2013). Larsen *et al*. (2017) reported that the salinity of groundwater is influenced by the presence of Holocene seawater trapped in the aquifer.

In order to monitor seawater intrusion, several methods have been reported. Martínez-Pérez *et al*. (2022) monitored the saltwater intrusion in the aquifer using integrated approach including the use of physical and chemical water analysis. The geophysics method assisted in identifying alternating of silt layers and their continuity (Kumar *et al*., 2022). The use of geoelectrical resistivity survey is also common in the exploration of seawater intrusion (Islami & Irianti, 2021). In addition, hydraulics tests can be used to check the tidal response (Crestani *et al*., 2022).

The use of the geoelectrical resistivity method has also been successfully used to map shallow aquifers in the coastal area (Thapa *et al*., 2019; Azizah *et al*., 2019). Abdulameer *et al*. (2018) reported that the geoelectrical resistivity method has been successful in mapping the possibility of seawater intrusion in southern Iraq. In general, research results that have been published to this day state that geoelectrical resistivity has been able to show the presence of brackish water and saltwater in the aquifer. However, there are no research results using geoelectrical resistivity that provide direct information on the prediction of the percentage content of seawater mixed with fresh water in the aquifer that is intruded by seawater. In this study, a correlation approach was used to determine the possible percentage of the presence of seawater mixed with fresh water in the aquifer. Thus, it is possible that the percentage of seawater mixed with fresh water can be predicted directly using the geoelectrical resistivity method.

0126-6187; 2637-109X / Published by the Geological Society of Malaysia.
© 2023 by the Author(s). This is an open access article distributed under the terms of the Creative Commons Attribution (CC-BY) License 4.0.

STUDY AREA

This research is a case study conducted in the coastal area around Dumai City, Indonesia. The locations chosen for field data collection were in several randomly selected sites in peat areas and also non-peat areas around the city of Dumai. Dumai is located in the coastal area which is directly adjacent to the Rupat Strait which is part of the Malacca Strait. It is precisely located in the Central Sumatra Basin where almost thirty percent of the land surface is covered by peat soil. The thickness of the peat soil in the Sumatran basin varies from about half a meter to about 7 m. The aquifer system in the Dumai area consisted of alternating of sand layer form the near surface to about 200 m depth (Anda *et al*., 2021). In the area around the Dumai, peat soils dominate in the coastal areas, especially in the eastern part of the Dumai up to about a few kilometers to the south of the Dumai city. However, in some places in the Southwest, the soil surface is dominated by clastic sediments. Figure 1 is a map of the research area. On this map, the elevation contours are presented with colored line. The white line is the resistivity survey line, while the yellow box is the location of the soil sampling, and the turquoise circle is the water sample location.

METHODOLOGY

In this study, several procedures were carried out to acquire the final target. The research was commenced from soil characterization, followed by sea-fresh water chemical analysis, resistivity measurement of seawater mixed with freshwater variations, measurement of soil resistivity saturated with various mixtures of sea-fresh water, and finally, measurements of geoelectrical resistivity and percentage of seawater in the intruded aquifer were conducted in the field.

Soil characterization

Soil samples were taken from a number of locations as shown in Figure 1. For each location, two packets of weight about 1 kg of soil samples were taken. All soil samples were measured with standard method (Teixeira & Martins, 2003). The first package was used to find the grain size of the soil that was referred to Hamlin (1991). They consist of clay, fine sand, medium sand, coarse sand, and gravel. The second portion of the soil was used for the purposes of measuring soil resistivity data which was saturated with a mixture of seawater and freshwater later on.

Water sample analysis

All water samples were analyzed using standard methods (Clesceri *et al*., 1999). A number of three water samples with 500 ml each have been collected using water mineral bottle to analyze their in situ physical character analysis such as temperature, conductivity, total dissolved solids, pH, and conductivity. Besides, the water samples were

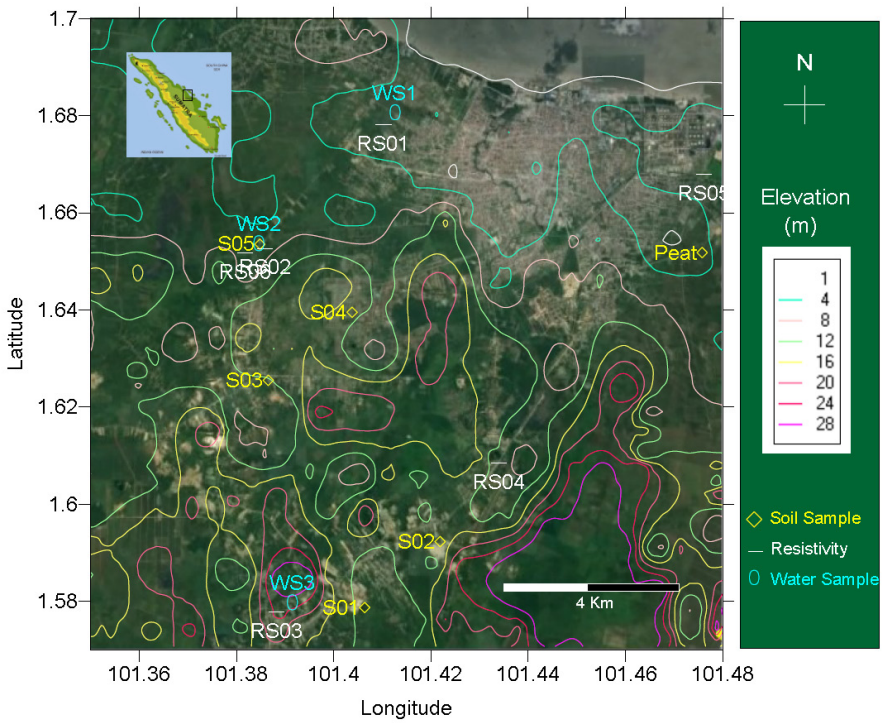

Figure 1: Map of the study area. The white line is the location of the geoelectrical resistivity survey. The yellow is the location of soil sample. The turquoise circle is the location of the water sample.

analyzed using Ion Chromatography (IC) and Inductively Coupled Plasma (ICP) to obtain their major anion and cation content such as Cl, SO_4, K, Ca, Mg, and Na. These chemical water sample data will be used to calibrate the geoelectrical resistivity survey later on.

Sea-fresh water chemical analysis

The seawater and sea-fresh water mixture were measured to obtain their major chemical content. The freshwater sample was obtained from the existing well which was located about 15 km from the beach line. The well is elevated 16 m above mean sea level while it's depth is 12 m from the ground surface. This well was chosen because it should be impossible to be intruded by seawater. In the laboratory, the analysis of sea-fresh water mixture with 0%, 5%, 10%, 25%, 50%, 75%, and 100% of seawater content was measured for their major chemical content.

Direct resistivity measurement of soil saturated with sea-fresh water mixture

The soil samples were saturated with the sea-fresh water mixture. The direct resistivity measurements were carried out in the laboratory on the entire saturated soil samples using the Wenner configuration with 0.05 m electrode spacing. These resistivity values obtained from the measurements were used as a reference in interpreting the geoelectrical resistivity data later so that the percentage of seawater content mixed with freshwater in the aquifer can be predicted through interpretation of geoelectrical resistivity survey data.

Geological and resistivity calibration

A new well was drilled to obtain the real geological data in the research area. These well data were used as calibration between geological and resistivity data. The well location was chosen in the community area. The soil samples were collected at every meter during the drilling process. The soil samples obtained from this well were also used to measure the resistivity value of soil saturated with sea-fresh water mixture.

Geoelectrical resistivity survey

In the field, 1D and 2D geoelectrical resistivity surveys were conducted using the Wenner configuration due to it give more signal strength (Telford *et al*., 1990) and less time for data acquisition (Loke, 2013). The homemade resistivity meter equipment was used with a maximum output current and voltage of 1 Ampere and 1000 Volt DC. Geoelectrical resistivity surveys were carried out at several sites. It started at about 300 m from the coastline to 10 km landwards. Thus, changes in the subsurface resistivity character can be clearly observed later. Both the 1D and 2D geoelectrical resistivity data were processed using Res1D and Res2DInv software by Loke (Loke *et al.,* 1996; Loke, 2001; Loke, 2013), respectively. The geoelectrical resistivity data were then interpreted based on direct soil measurements of data of the saturated sea-fresh water mixture. Thus, the percentage of seawater content in the aquifer can be known through resistivity measurements on the surface.

RESULTS AND DISCUSSION

Soil grain size sample

The grain size distributions of the soil samples obtained from the study area are given in Table 1. The grain size data in the table is from the soil of clastic sediment samples only. For tpeat, particle size measurements were not carried out. In the table, it can be observed that no gravel was found in the soil sample. Soil samples for S01 to S04 were dominated by silt and clay which were taken from a depth of 1 m. While samples S05 and S06 are dominated by fine sand and medium-size sand taken from the new wells drilled in this study.

Chemical content of seawater freshwater mixtures

Table 2 shows the main chemical content of seawater mixtures. In the table, the standard chemical content of seawater was placed in the last row of the table. These values were obtained from Hounslow (1995). Cl is the highest concentration in each of the water samples, followed by sodium and SO_4. In a water sample of 5% seawater mixture (AL05), the Cl concentration is detected as much as 498

Table 1: Grain size of the soil in the selected locations of the study area.

Sample No	Sampling Depth (m)	Silt and Clay (%)	Fine Sand (%)	Medium Sand (%)	Coarse Sand (%)	Gravel (%)
S01	1	94.7	2.3	3.0	0.0	0
S02	1	94.7	2.3	2.9	0.0	0
S03	1	96.0	1.0	2.9	0.1	0
S04	1	91.5	1.0	7.1	0.4	0
S05	16	0.4	52.0	40.2	7.4	0
S06	20	0.3	16.5	59.7	23.3	0

Table 2: Chemical analysis of water sample. The water sample is varied with the seawater content. The standard value of seawater content derived from Hounslow (1995) is placed at the last row of the table.

Sample ID	Seawater (%)	Cl (mg/L)	SO_4 (mg/L)	K (mg/L)	Ca (mg/L)	Mg (mg/L)	Na (mg/L)
AL00	0	11	5	2.3	11.3	0.7	2.3
AL05	5	498	79	29.0	25.2	50.2	Sat
AL10	10	1185	162	57.9	37.6	87.6	Sat
AL25	25	4057	227	115.5	88.4	264.3	2487.1
AL50	50	7444	868	192.2	186.5	654.4	4882.3
AL75	75	10616	1184	298.4	284.3	995.9	7944.0
AL100	100	16712	1938	378.3	398.8	1272.0	10687.5
Hounslow	Seawater	19000	2700	390	410	1350	10500

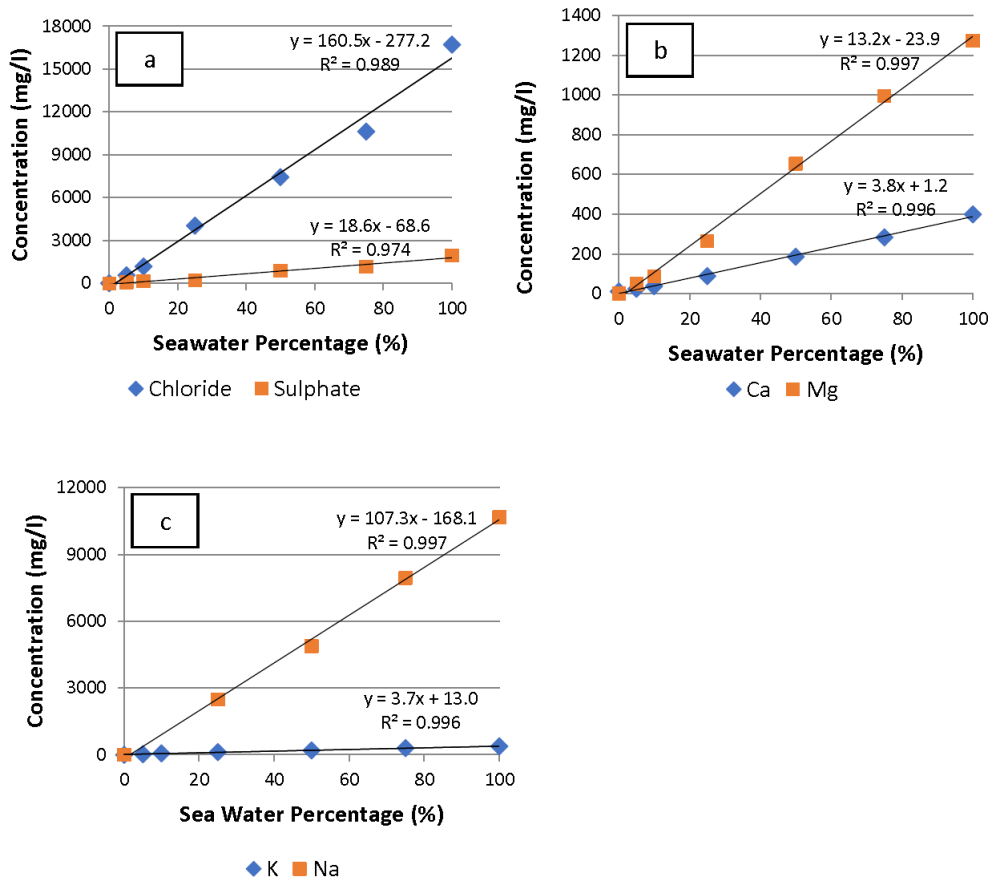

Figure 2: Water chemical content varies with the percentage of seawater, (a). Cl and 192 SO_4, (b). Ca and Mg (c). K and Na.

mg/L. Whilst the concentration of Cl is 16712 mg/L in the seawater (AL100). Figure 2 is the scatter plot of data in Table 2 that shows a correlation between the percentages of seawater content and the chemical content. It is obvious that the Cl concentration upsurges linearly in line when the percentage of seawater content increase (AL00-AL100). The other major seawater chemical components (SO_4, K, Ca, Mg and Na) too have the same linear trend with the Cl. All the chemical concentrations have a high correlation (R^2 value) with a value near 1. This suggests that the measurement of the chemical and the trend of seawater percentage are precise and accurate.

Resistivity and soil property correlation

Direct resistivity measurements on soils saturated with seawater and a combination of a mixture of seawater and freshwater can be seen in Table 3. Whilst, Figure 3 is the data in Table 3 plotted using bar chart (Figure 3A). In Figure 3A it can be seen that the resistivity of the soil which is only saturated with freshwater shows a relatively high compared to all soil samples. The soils dominated by sand have relatively high resistivity value compared to soils dominated by silt and clay. For soils that are dominated by silt and clay, the amount of resistivity does not show too much difference. This is because each soil has relatively the

Table 3: Direct resistivity measurement of the seawater variation saturated soil.

Sea-water (%)	S01 (ohm.m)	St. dev	S02 (ohm.m)	St. dev	S03 (ohm.m)	St. dev	S04 (ohm.m)	St. dev	S05 (ohm.m)	St. dev	S06 (ohm.m)	St. dev	Peat (ohm.m)	St. dev
0	49.2	0.5	47.1	0.4	44.4	0.3	45.7	0.4	108.6	0.02	113.4	0.04	136.1	2.3
5	11.8	0.28	11.5	0.02	10.9	0.02	11.1	0.02	19.9	0.01	20.0	0.01	22.4	0.8
10	6.9	0.03	7.0	0.02	6.7	0.02	6.8	0.02	11.5	0.02	12.1	0.03	12.9	0.03
25	5.4	0.03	5.1	0.02	4.9	0.02	4.9	0.02	9.1	0.01	9.4	0.08	9.9	0.04
50	2.9	0.06	2.5	0.01	2.4	0.01	2.4	0.01	4.8	0.01	4.9	0.01	5.1	0.06
75	1.3	0.07	1.2	0.02	1.2	0.03	1.2	0.01	2.3	0.01	2.4	0.03	2.6	0.01
100	0.9	0.04	0.8	0.01	0.8	0.01	0.6	0.01	1.7	0.01	1.8	0.03	1.9	0.2

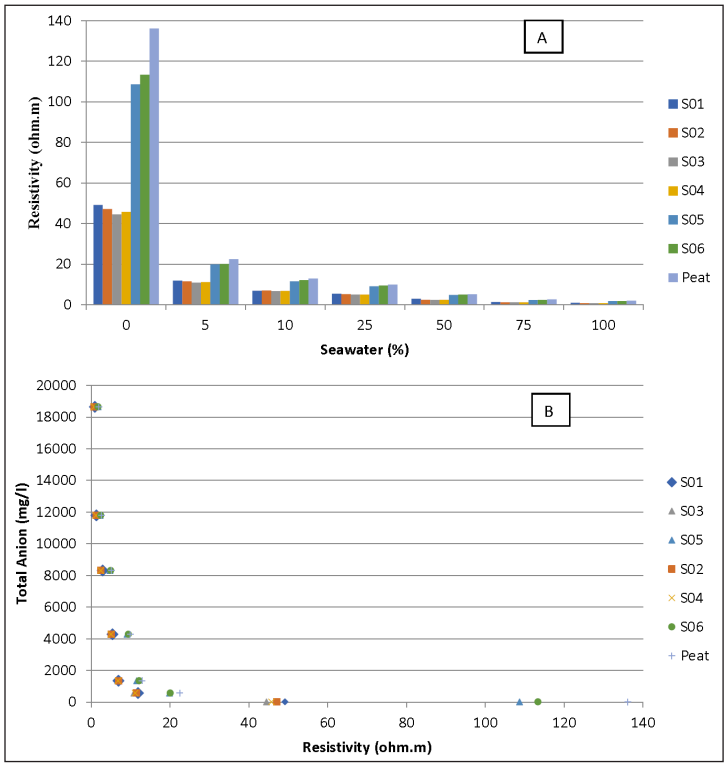

Figure 3: Resistivity and percentage of seawater in the soil sample (Figure 3A). Total anion 227 and resistivity of saturated soil with different seawater content (Figure 3B). In Figure 3B, the 228 resistivity value decreases drastically when increasing a little bit of seawater content.

same grain character, except for peat soil, the resistivity of peat soil containing freshwater has the highest resistivity value (136 ohm.m) compared to other soils. In the soil sample filled with a mixture of 25% sea-fresh water, it is seen that the overall resistivity drops drastically to around 10-22 ohm.m. It is also seen that the peat sample also has the highest resistivity value (22 ohm.m) as in the soil saturated with fresh water. This is because the soil has organic content from trees that have been destroyed.

The same trend of resistivity value is also observed for 50% of the sea-fresh water mixture, as in soil of 25% and 10% seawater content. In general, the resistivity value in the sample with 50% seawater content is slightly lower than the previous 25% resistivity. Likewise, it is also observed in the resistivity value of the sample with a seawater content of 75% and also 100%.

Figure 3(B) is showing the total anions in the water sample that is used to saturate the soil sample. It can be seen that the addition of 5% seawater into freshwater causes the resistivity value to drop drastically. This is because the anion content in the water will increase the conductivity value of a material drastically. Thus the resistivity value will drop drastically as well. However, the decrease in the resistivity value is not linear but is exponential until the seawater content becomes 100%.

Calibration and geoelectrical resistivity survey

To calibrate the interpretation of 1D and 2D geoelectrical resistivity data against geological data, a new well was drilled near the housing of one of the residents, and the well can be used by the community in the future for daily uses. Figure 4 is the drilling process and also the lithology

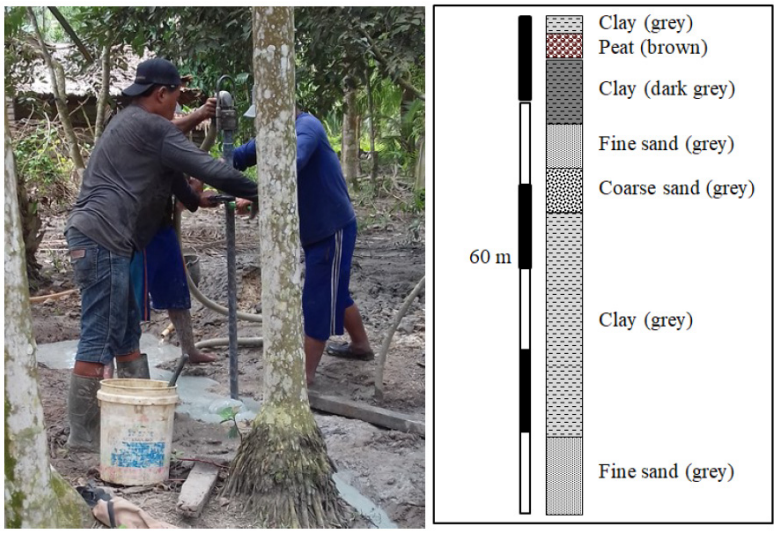

Figure 4: Drilling process in WS2 (left) and lithology log of the well WS2 (right).

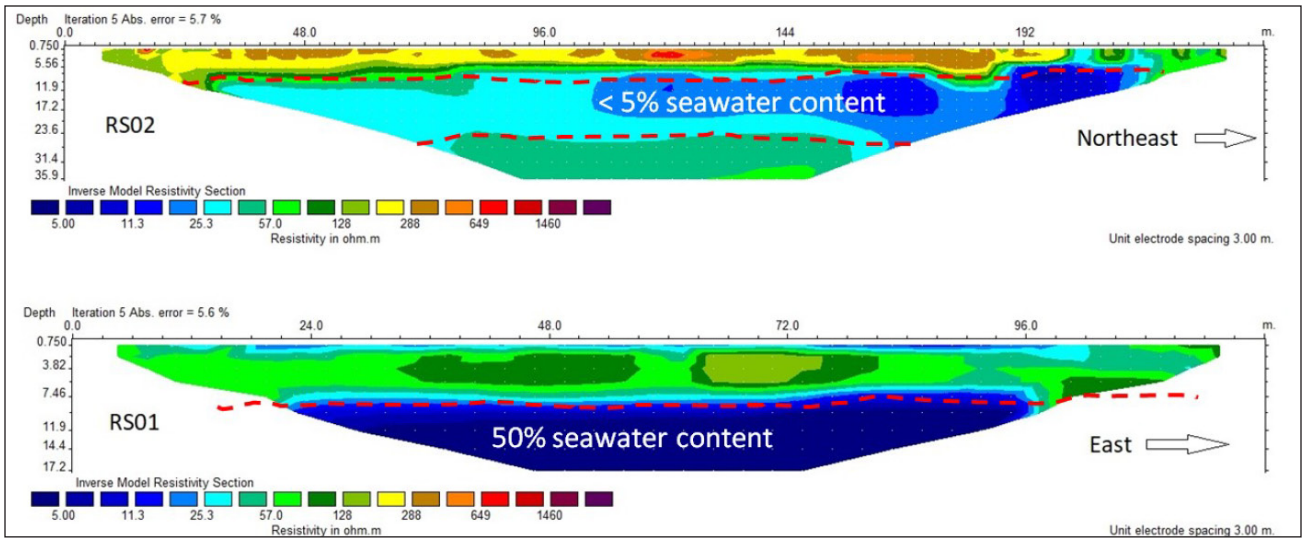

Figure 5: 2D Geoelectrical resistivity model.

log obtained from the collection of soil samples during the drilling process. During drilling, soil samples were collected and observed for every 1 m. In this well, from the surface to a depth of 90 cm is embankment soil, then peat soil with dark brown color was found to a depth of 5 m. After that, clay soil with a dark gray color was found to a depth of 13 m. From a depth of 13 m to 18 m, it is dominated by fine gray sand then coarse sand to a depth of 24 m. The depth zone ranging from 13 m to 24 m is the first aquifer zone that is often used for groundwater extraction by the community. During the soil collection, at a depth of about 18-24 m, when collecting this coarse-grained sand, the sand is slightly reddish when it was exposed to the surface after a few hours. After a layer of coarse sand, followed by a layer of gray clay from a depth of 24 m to 50 m, there were several color changes but were not too pronounced. The last layer is fine gray sand from a depth of 50 to the end of the maximum depth of the well (60 m).

Figure 5 is a geoelectrical resistivity model that was carried out at about 100 m next to the new drilled well. It was conducted exactly at the mark of 84 m on the RS02. In this model, it can be seen that on the X-axis is the position of the electrode while on the Y-axis is the depth of the data inversion model results. The model was generated in the inversion process using the Res2DInv software. It shows that the upper surface is dominated by yellow color with a resistivity value of around 180 ohm.m. This value is associated with peat in the vadose zone. While at the next depth of about 5 m to about 12 m, the resistivity value is dominated by around 70 ohm.m. This value is interpreted as a clay zone that is dark gray in color. Next, the resistivity value is around 40 ohm.m (turquoise color). This color can be observed from a depth of 12 m to about 25 m. This zone is correlating to an aquifer zone. The aquifer consists of sand containing freshwater that has been slightly mixed (less than 5%) of seawater. This interpretation is based on the data in Table 3 that for sandy soils saturated with 5% seawater, the resistivity value is about 20 ohm.m. In addition, this interpretation is also supported by the water chemical data at W2 (Table 4) which is about 100 m from the line of the geoelectrical resistivity survey. In the table, the Cl content of the groundwater for W2 is 276 mg/l with the salinity of 0.2%. This value is indicating that the aquifer contains less than of 5% seawater content mixed with freshwater.

The geoelectrical model of resistivity RS01 can be seen in Figure 5. The geoelectrical resistivity survey of RS01 was conducted on the grass field of farm animals such as cows and goats. The resistivity model shows that the resistivity value is about 15 ohm.m on the surface. This value correlates to the wet zone soil contaminated with the farm animal's manure. The next layer shows the resistivity value of about 70 ohm.m correlating to the clay layer. The shallow aquifer appears from a depth of 7 m downward. The resistivity value of this layer is less than about 5 ohm.m. The resistivity extraction also gave information at this zone the lowest resistivity value is 3 ohm.m. Based on the resistivity value and the data in Table 3, the percentage of seawater mixed with the freshwater here is about 25% until 50%. This quantitative interpretation is also supported by the well WS1 (50 m from the survey line) which the Cl content of the groundwater is 1798.5 mg/l (Table 4). The resistivity value of seawater intrusion in the aquifer is also appeared about 5-10 ohm.m as reported in Sun *et at*. (2022) and Niculescu *et al.* (2021).

The results of the 1D modeling of the geoelectrical resistivity survey data in this study can be seen in Figure 6. In this 1D model, the observed data and calculated data as well as the resistivity model with depth prediction can be seen in the given model. The geoelectrical resistivity model RS06 was deliberately carried out at the same location as RS02 (2D geoelectrical resistivity data) to view and calibrate 1D data with 2D data controlled by well lithology log data. In the RS06 geoelectrical model, it can be seen that they are 4 layers of resistivity zones. From the surface to a depth of approximately 5 m, the resistivity value is around 180 ohm.m. This zone is interpreted as a vadose zone. The next resistivity layer is a zone that has a resistivity value of about 110 ohm.m w hich correlates to the clay zone. Then at a depth of about 11 m to 25 m, another layer is observed that has a resistivity value of about 23 ohm.m. This zone is a shallow aquifer zone. This aquifer zone like RS02 is also confirmed from the lithology log data of the wells made in this study (Figure 4), which shows that this depth range is dominated by fine sand and coarse sand. From the results of 1D geoelectrical resistivity (RS06) and 2D geoelectrical resistivity (RS02) data which were carried out at the same place, it is seen that both of them show almost the same resistivity pattern at a certain depth.

Table 4: Wells physical *in-situ* data, major anion and cation data.

Well ID	Depth (meter)	pH	Salinity 0/00	TDS mg/l	Cl mg/l	SO_4 mg/l	K mg/l	Ca mg/l	Mg mg/l	Na mg/l	Fe mg/l
WS1	15	7.4	1.1	3260	1798.5	470.2	2.3	73.6	48.8	67.4	0.3
WS2	18	6.9	0.2	792	276.9	69.6	1.5	44.5	21.4	10.2	3.8
WS3	12	6.7	0	163	63.9	12.6	1.3	15.2	3.2	22.2	0.7

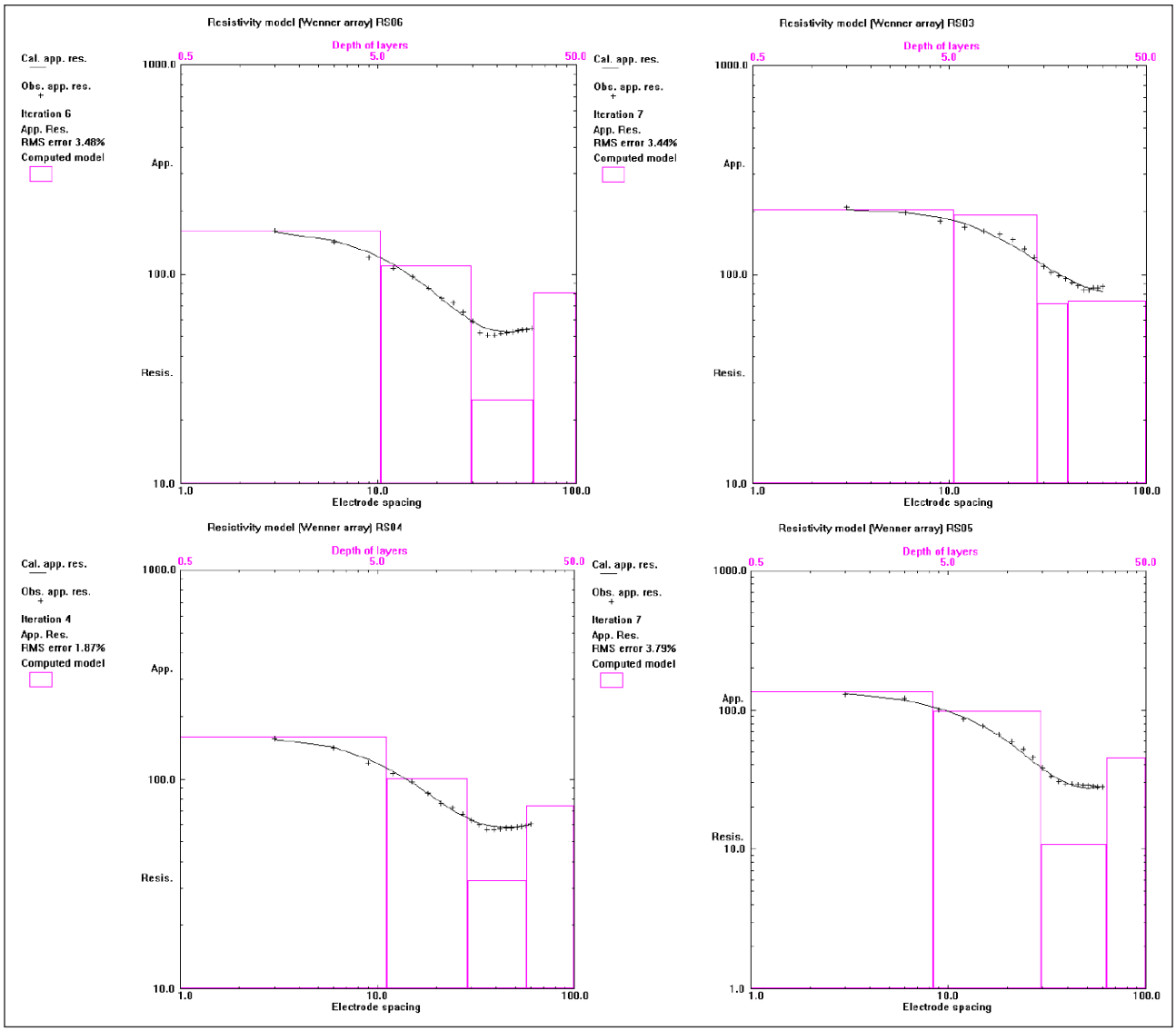

Figure 6: 1D geoelectrical resistivity model.

The 1D geoelectrical resistivity model for RS03, RS04, and RS05 can be seen in Figure 6. In RS03 no zone has a low resistivity value. In this model, a shallow aquifer is seen at a depth of approximately 11 m until approximately 22 m with a resistivity of about 80 ohm.m. This means that the shallow aquifer at this location does not indicate of the presence of seawater. This is also proven by the groundwater samples in this site (W3) which have 0% salinity and relatively low Cl (63.9 mg/l). For RS04, in the aquifer zone, there is also no visible presence of seawater in the aquifer. This interpretation is based on the fact that in the aquifer zone, the resistivity value is about 60 ohm.m, this means that according to Table 3, the aquifer is filled with freshwater without any mixture with seawater. While in RS05, the presence of seawater is around 25% very clearly visible. It can be seen in the aquifer zone that the resistivity value is about 8 ohm.m. By knowing the soil character and also the amount of soil resistivity that is saturated with various types of seawater mixtures in freshwater, thus a quantitative interpretation of the percentage of seawater content mixed in the aquifer can be predicted from geoelectrical resistivity data, both 1D and 2D.

CONCLUSION

This research has successfully shown how to interpret geoelectrical resistivity data quantitatively, especially in the coastal area with seawater intrusion problems in the aquifer. Comprehensive investigations of soil characteristics, chemical analysis, and direct resistivity measurement have been done in the Dumai area. The main conclusion can be stated as the followings:

1. The grain size of the soil is affecting the resistivity reading of the soil. Increasing the sand content in the

soil will have a positive correlation with the reading of soil resistivity value.

2. The geoelectrical resistivity value of the soil saturated with a different salt-fresh water mixture has a good correlation with the pore soil content in the aquifer. Resistivity value decreases drastically with increasing a little bit of seawater content. The anion content of the water in the pore soil is the main factor affecting in the lowering of the resistivity reading of the soil.
3. The decreasing of resistivity value in the soil saturated by the salt-fresh water mixture shows an exponential shape as increasing seawater content in the pore soil. The quantitative interpretation of seawater intrusion in the aquifer can be done through the resistivity data.
4. The groundwater in the shallow aquifer of the study area has variation in the percentage of seawater content. It was found that 50% of saltwater mixed with the fresh water in the aquifer around 500 m from the coastal line. Whilst, in the landward of about 5 km from the coastal line, the saltwater is about 25% in the aquifer.
5. The limitation of study should be imposed that the study valid in sand and gravel medium compared to clay due to soil chargebility.

ACKNOWLEDGMENTS

Thank you to the DRPM through the LPPM Universitas Riau for the research funding number: 1609/UN19.5.1.3/PT.01.03/2022. We are also very grateful to the reviewers and editor for valuable comments.

AUTHOR CONTRIBUTIONS

NI: designing the research, coordinating the team, data interpretation, writing the article. MI: Analyzing the groundwater samples. AA: Collecting ID resistivity data. MN: 1D resistivity processing. MN: Collecting 2D resistivity data. FF: 2D resistivity processing. DI: Compiling files and helped in writing article.

CONFLICT OF INTEREST

The authors declare that there is no conflict of interest regarding the publication of this article

REFERENCES

Abdulameer, A., Thabit, J. M., AL-Menshed, F. H. & Merkel, B., 2018. Investigation of seawater intrusion in the Dibdibba Aquifer using 2D resistivity imaging in the area between Al-Zubair and Umm Qasr, southern Iraq. Environ Earth Sci., 77, 1-15. https://doi.org/10.1007/s12665-018-7798-3.

Alfarrah, N. & Walraevens, K., 2018. Groundwater overexploitation and seawater intrusion in coastal areas of arid and semi-arid regions. Water, 10 (2), 143. https://doi.org/10.3390/w10020143.

Anda, M., Ritung, S., Suryani, E., Hikmat, M., Yatno, E., Mulyani, A. & Subandiono, R. E., 2021. Revisiting tropical peatlands in Indonesia: Semi-detailed mapping, extent and depth distribution assessment. Geoderma, 402, 115235. https://doi.org/10.1016/j.geoderma.2021.115235.

Armanuos, A.M., Moghazy, H.E., Zeleňáková, M. & Yaseen, Z. M., 2022. Assessing the impact of groundwater extraction on the performance of fractured concrete subsurface dam in controlling seawater intrusion in coastal aquifers. Water, 14(13), 2139. https://doi.org/10.3390/w14132139.

Azizah, N., Pratiwi, N.H., Islami, A.P. & Islami, N., 2019. Application of geoelectrical resistivity methods for mapping of seawater intrusion. Journal of Physics: Conference Series (Vol. 1351, No. 1, p. 012094). IOP Publishing. https://doi.org/10.1088/1742-6596/1351/1/012094.

Baharuddin, M.F.T., Taib, S., Hashim, R., Abidin, M.H.Z. & Rahman, N.I., 2013. Assessment of seawater intrusion to the agricultural sustainability at the coastal area of Carey Island, Selangor, Malaysia. Arabian Journal of Geosciences, 6(10), 3909-3928. https://doi.org/10.1007/s12517-012-0651-1.

Basack, S., Loganathan, M. K., Goswami, G. & Khabbaz, H., 2022. Saltwater intrusion into coastal aquifers and associated risk management: Critical review and research directives. Journal of Coastal Research, 38(3), 654-672. https://doi.org/10.2112/JCOASTRES-D-21-00116.1.

Clesceri, L.S., Greenberg, A.E. & Eaton, A.D., 1999. Standard methods for the examination of water and wastewater. American Public Health Association, AWWA and Wat. Environ. Fed., 1134 p.

Crestani, E., Camporese, M., Belluco, E., Bouchedda, A., Gloaguen, E., & Salandin, P., 2022. Large-scale physical modeling of salt-water intrusion. Water, 14(8), 1183. https://doi.org/10.3390/w1408118.

Erostate, M., Huneau, F., Garel, E., Ghiotti, S., Vystavna, Y., Garrido, M. & Pasqualini, V., 2020. Groundwater dependent ecosystems in coastal Mediterranean regions: Characterization, challenges and management for their protection. Water Research, 172, 115461. https://doi.org/10.1016/j.watres.2019.115461.

Hamlin, W.K., 1991. Earth Dynamic Systems (6th ed.). Bringham Young University, Provo, Utah. 924 p.

Hounslow, A.W., 1995. Water quality data: Analysis and interpretation. Lewis Publishers. U.S. 397 p.

Islami, N., & Irianti, M., 2021. Resistivity characteristics of soil saturated with variation of salt water-fresh water mixture. Journal of Physics: Conference Series (Vol. 2049, No. 1, p. 012029). IOP Publishing.

Kumar, P., Tiwari, P., Biswas, A. & Acharya, T., 2022. Geophysical investigation for seawater intrusion in the high-quality coastal aquifers of India: A review. Environmental Science and Pollution Research, 1-37. https://doi.org/10.1007/s11356-022-24233-9.

Larsen, F., Tran, L.V., Van Hoang, H., Tran, L.T., Christiansen, A.V., & Pham, N.Q., 2017. Groundwater salinity influenced by Holocene seawater trapped in incised valleys in the Red River delta plain. Nature Geosci., 10, 376–381. https://doi.org/10.1038/ngeo2938.

Loke, M.H., 2001. RES1D version 1.0 for Windows 95/98/Me/2000/NT. 1-D Resistivity, IP & SIP Inversion and forward modelling for Wenner and Schlumberger arrays. 178 p.

Loke, M.H., 2013. Tutorial : 2-D and 3-D electrical imaging surveys. Geotomo Softw. Malaysia. 232 p.

Loke, M.H. & Barker, R.D., 1996. Rapid least-squares inversion of apparent resistivity pseudosections by a quasi-Newton method. Geophys. Prospect. https://doi.org/10.1111/j.1365-2478.1996.tb00142.x.

Martínez-Pérez, L., Luquot, L., Carrera, J., Marazuela, M.A., Goyetche, T., Pool, M., & Folch, A., 2022. A multidisciplinary approach to characterizing coastal alluvial aquifers to improve understanding of seawater intrusion and submarine groundwater discharge. Journal of Hydrology, 607, 127510. https://doi.org/10.1016/j.jhydrol.2022.127510.

Niculescu, B.M. & Andrei, G., 2021. Application of electrical resistivity tomography for imaging seawater intrusion in a coastal aquifer. Acta Geophysica, 69(2), 613-630. https://doi.org/10.1007/s11600-020-00529-7.

Panthi, J., Pradhanang, S.M., Nolte, A. & Boving, T.B., 2022. Saltwater intrusion into coastal aquifers in the contiguous United States - A systematic review of investigation approaches and monitoring networks. Science of the Total Environment, 155641. https://doi.org/10.1016/j.scitotenv.2022.155641.

Prusty, P. & Farooq, S.H., 2020. Seawater intrusion in the coastal aquifers of India-A review. HydroResearch, 3, 61-74.

Sun, J.H., Cheng, L.Q., Zhao, W.F., Ren, G.J., Sun, G.S., Wang, R.P. & Pei, M.X., 2022. Relationship between apparent resistivity and chloride ion concentration in seawater intrusion areas: A case study of Qinhuangdao. Geophysical and Geochemical Exploration, 46(2), 518-524. https://doi: 10.11720/wtyht.2022.1220.

Teixeira, W.G. & Martins, G.C., 2003. Soil physical characterization. Amazonian Dark Earths: Origin Properties Management, 271-286.

Telford, W.M., Geldart, L.P. & Sheriff, R.E., 1990. Applied Geophysics, Cambridge University Press, 77 p.

Thapa, B.R., Shrestha, S.R., Okwany, R.O. & Neupane, M., 2019. Shallow aquifer potential mapping in the foothills of Churia in Eastern Gangetic Plain of Saptari District, Nepal. Appl. Water Sci., 9, 92. https://doi.org/10.1007/s13201-019-0971-3.

Manuscript received 9 June 2022;
Received in revised form 23 February 2023;
Accepted 7 March 2023
Available online 26 May 2023